*Solid State Phenomena Vol. 105 (2005) pp. 385-390*
*online at http://www.scientific.net*


# Combined analysis of Bi2223 superconducting bulk materials

E. Guilmeau[1, a], D. Chateigner [2,b], J. Noudem[2] and B. Ouladdiaf[3]

[1]National Institute of Advanced Industrial Science and Technology, Midorigaoka, Ikeda, Osaka 563-8577, Japan

[2]CRISMAT-ENSICAEN Laboratory, UMR CNRS 6508, 6 Bd. Maréchal Juin, 14050 Caen Cedex, France

[3]ILL, BP 156, 38042 Grenoble, France

[a]e-guilmeau@aist.go.jp, [b]daniel.chateigner@ismra.fr

**Keywords:** texture, superconductor, Bi2223, combined analysis.

**Abstract.** Orientation distributions of polyphased $(Bi,Pb)_2Sr_2Ca_2Cu_3O_{10+\delta}$ superconducting textured materials are determined from neutron diffraction analysis. The quantitative texture analysis of neutron data was accomplished by using the combined Rietveld-WIMV-Popa algorithms, implemented in the program package Materials Analysis Using Diffraction (MAUD). Curved position-sensitive detector and 4-circle diffractometry allow the whole diffraction pattern treatment. Transport critical current densities, measured on different samples, are strongly dependent of the calculated texture strengths, crystallite sizes and phase ratios. The results prove the interest of the combined approach for a quantitative texture analysis of complex materials. Texture to anisotropic physical properties relationship is discussed.

## Introduction

The controlled development of texture in polycrystalline materials appears to be more and more essential in ceramic processing, since potential applications require materials with macroscopic properties comparable to the anisotropic properties of the crystal structures. Texture analysis is consequently recognized as a really important tool in the characterisation of oriented ceramics. However, a quantitative texture analysis of these materials is usually not a simple task. In most cases, the diffraction spectra are very complex with many partially or fully overlapping diffraction peaks and with several crystallographic phases. The X-ray defocusing effect limits also the pole figure coverage and obstructs the analysis. To overcome this problem, the combination of Rietveld [1], WIMV [2] and Popa [3] approaches, for instance as implemented in the MAUD software [4] (Materials Analysis Using Diffraction), permits a comprehensive new approach to crystal structure-texture-microstructure analysis. The increasing number of papers, based on such kind of methodology, illustrates the interest of many researchers in materials science to the combined analysis [5-10]. In this study, we report the application of this method to polyphased $(Bi,Pb)_2Sr_2Ca_2Cu_3O_{10+\delta}$ materials with different textures, crystallographic structures, microstructures….Orientation distributions (OD) were determined from neutron diffraction on curved position-sensitive detectors. We demonstrate the efficiency and reliability of iterative combination of algorithms for structure determination (Rietveld), microstucture (Popa) and OD calculation (WIMV) in the case of oxide ceramic materials. Correlation between texture strengths and superconducting current densities is illustrated.

## Experimental

The analysed samples are mixtures of two superconducting phases, $(Bi,Pb)_2Sr_2Ca_2Cu_3O_{10}$ (Bi2223), $(Bi,Pb)_2Sr_2CaCu_2O_8$ (Bi2212), and one alkaline earth cuprate phase $(Sr,Ca)_{14}Cu_{24}O_{41}$ (14:24) in a residual content. Four samples were prepared by the newly developed Calcination-Sinter-Forging method (CSF) [11] using 20, 50, 100 and 150 h of sinter-forging dwell-times, respectively. Starting

from calcined powders composed of Bi2212 and secondary phases such as $Ca_2PbO_4$, $Ca_2CuO_3$ or CuO, the thermomechanical treatment (temperature and uniaxial pressure) allows simultaneously the nucleation and growth of the Bi2223 phase and the alignment of both Bi2212 and Bi2223 plate-like grains. The initial isotropic microstructure of the sintered material (Fig. 1a), in terms of crystallographic orientations, is modified into a preferential orientation of the grains (Fig. 1b). The resulting superconducting phases are strongly textured with their mean c-axes parallel to the pressure direction and consequently perpendicular to the disc surface. The increase of the sinter-forging dwell time is performed here in order to obtain a material composed of the highest content in Bi2223 and, consequently, to improve superconducting properties. The grain alignment is also crucial in order to optimize the anisotropic transport properties of our materials.

The specimens were analyzed on the D1B neutron line at the Institut Laüe Langevin, Grenoble. The neutron wavelength is monochromatised to $\lambda$=2.523 Å. Diffracted neutrons are collected by a curved detector composed of 400 cells spread over 80° (resolution 0.2°) in 2$\theta$. An Eulerian cradle allows the $\chi$ angle rotations. Scans were operated from $\chi$ = 0 to 90° (step 5°) using a fixed incidence angle $\omega$ of 19.84°. The average volume of our samples is around 25mm$^3$, this corresponding to measuring times around 20 mn per sample orientation.

The transport critical current densities ($J_c$) were measured on superconducting samples by the standard four-probe technique at 77K with an electric field criterion of 1µV/cm. The dimensions of the samples were approximately 10×1.5×0.2 mm$^3$, in the same order of magnitude to the volume probed in neutron experiments.

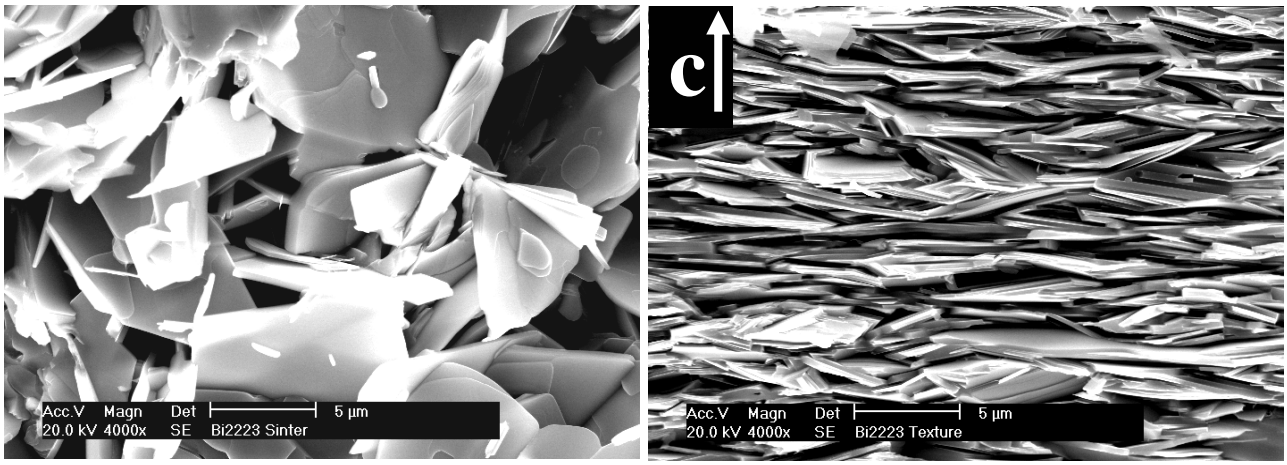


*Fig. 1: SEM micrographs of (a) sintered ceramics without preferential orientation and (b) sinter-forged ceramics with mean c-axes parallel to the pressure direction.*

## Results and discussion

The figure 2 illustrates the refinement reliability on a selection of 19 diagrams (0 to 90° $\chi$-scans) obtained typically on our samples. These spectra were measured on the sample textured during 150h at 845°C. In this case, only the Bi2212 and Bi2223 phases have been considered in the refinement. The introduction of the '14:24' phase in the refinement has been reported elsewhere [12]. This graph highlights clearly the (00$\ell$) texture of both Bi2212 and Bi2223 phases. In particular, we can clearly observe the disappearance of the (00$\ell$) lines when $\chi$ increases up to 30°, the appearance of (11$\ell$) lines for intermediate $\chi$ angles and the intensity increase of (200), (020) and (220) lines when $\chi$ tends to 90°.

One can appreciate the correct agreement between the experimental and refined spectra, which corresponds to RP, RP1, $R_w$ and $R_{Bragg}$ factors equal respectively to 16.2%, 12.25%, 9.12 and 6.13%. However, we can estimate that these values are still not optimized in reason of the problem of overlapping between (008) and (0010) or between (0012) and (0014) peaks of Bi2212 and

Bi2223, respectively, for $\chi$ positions closed to 0°. The origin of this phenomena is probably linked to stacking defects or intergrowth along the c-axis which induces new periodicities and diffraction peaks characterized by intermediate c parameters. However, we have not yet elucidated this question, and no algorithm is included to solve intergrowths in the combined approach. In spite of this problem, the calculated pole figures recalculated from the OD obtained by the WIMV algorithm (figure 3), illustrates well the (00l) texture of the material. Pole figures are related to Bi2223 phase in sample textured during 150h at 845°C. The {0010} pole figure exhibits a strong centred pole as a sign of the strong preferential orientation with c-axes parallel to the sample normal. The {115} pole figure presents a circle with maximum of distribution density stayed for $\chi$ position around 65°, value equal to the angle between (001) and (115) directions in the orthorhombic structure. Maximum of distribution density around $\chi$=90° for the {220} pole figure is also compatible with the theoretical texture and structure.

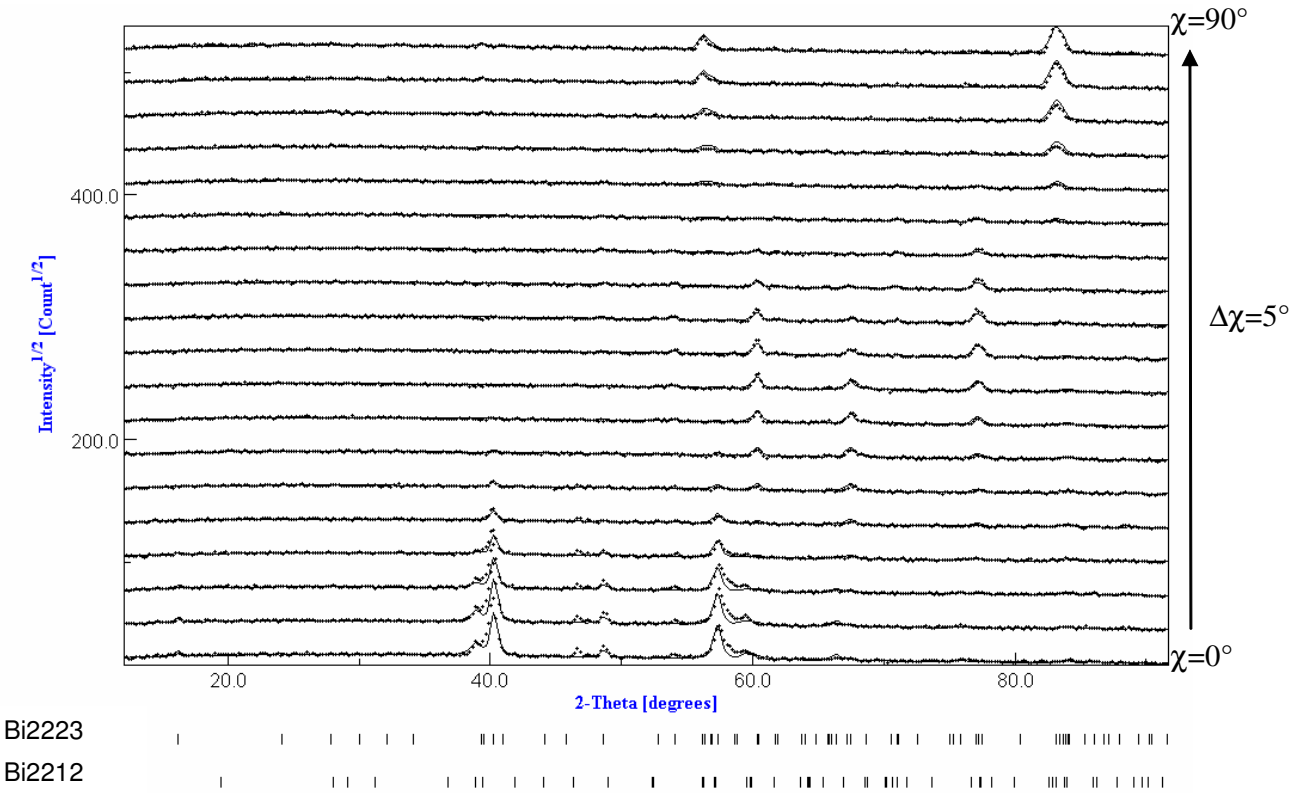


*Figure 2: Experimental and calculated neutron diffraction parttern for various $\chi$ positions (0 to 90°), 150h sinter-forged Bi2223 sample [12].*

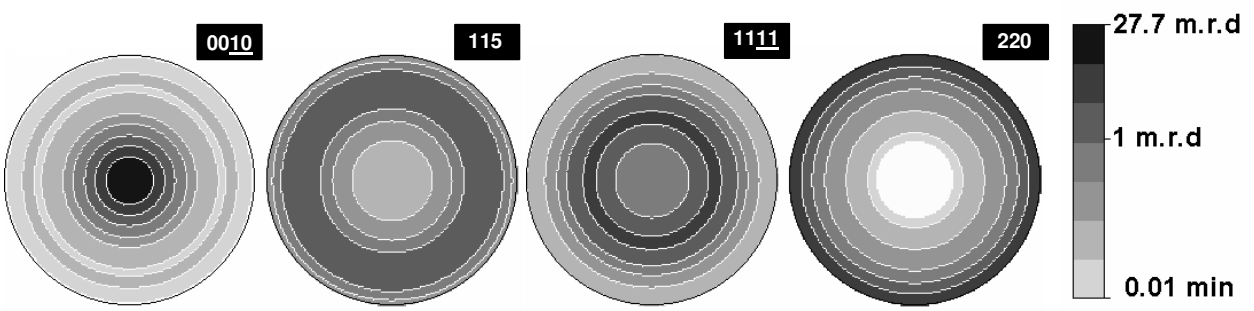


*Figure 3 : Selected {00$\underline{10}$}, {115}, {11$\underline{11}$} and {220} pole figures recalculated from the OD obtained by the WIMV algorithm. 150h sinter-forged Bi2223 sample. Logarithmic density scale, equal area projection.*

From the point of view of transport properties in the (ab) planes, it is really important to check which (hk$\ell$) planes align with their normal along **z** (normal to sample surface), which cannot be evidenced easily by only pole figures. The full representation of the OD is needed, which in the case of fiber textures can be represented by the inverse pole figure (figure 4) calculated for the **z** fiber direction. In this figure, we can retrieve the previously described (001) major component for all the four samples with a small component for (10$\ell$) and (hk0) planes, probably related to the overlapping problems for low $\chi$ positions. Nevertheless, these graphs confirm the development of the (00$\ell$) texture and highlights the increase of the texture strength for higher sinter-forging dwell-time.

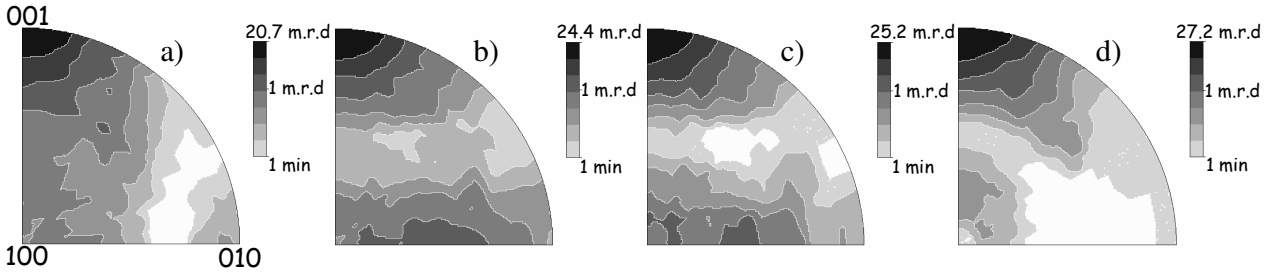


*Figure 4 : Inverse pole figures calculated for the direction normal to the sample planes (fiber axis of the texture). Samples textured during (a) 20h, (b) 50h, (c) 100h and (d) 150h. Logarithmic density scale, equal area projection.*

Finally, the table 1 summarises all the refined parameters (cell parameters, crystallite size, max of the {00$\ell$} orientation distribution *(ODmax)*, phase ratio) and reliability factors calculated from each sample analysis. Transport critical current densities, measured on each samples, are also reported in this table. It appears a clear correlation between the evolution of each refined parameter and the sinter-forging dwell-time. The improvement of bulk performances, *i.e.* the critical current densities ($J_c$), is closely related to an increase of the *ODmax*, the Bi2223 phase content and the crystallite size. The circulation of the current is not only facilitated by a better alignment of grains and a larger percentage of Bi2223 but also by a larger crystallite size which limits consequently the number of grain boundaries, so current barriers in the material. We can also note that, for a 20h and 50h dwell time, the textures of Bi2212 and Bi2223 are very closely linked indicating the strong growing interaction between these phases. The difference occuring for longer dwell times is due to an insufficient counting statistics which is not suitable to extract exact parameters related to the Bi2212 phase. It should be noted here, that a nucleation-growth mechanism between Bi2212 and Bi2223 phases, even for long dwell time, has been established in previous works [13]. In that case, X-ray analysis with a point detector and an important acquisation time are appropriate to measure via a direct quantitative analysis the textures of both Bi2212 and Bi2223 phases, and to show the link between the two textures even for sinter-forging dwell time equal to 100h and 150h.

*Table 1: Refined parameters extracted from Rietveld/WIMV combined analysis and reliability factors obtained from different sinter-forging time samples. Transport critical current densities, measured on each sample, are also reported in this table.*

| Sinter-forging dwell time [h] | Orientation Distribution Max [m.r.d.] | | % Bi2223 | Crystallite size Bi2223 [nm] | $R_{Bragg}$ (%) | Rw (%) | RP0 (%) | RP1 (%) | $J_c$ [A/cm$^2$] |
|---|---|---|---|---|---|---|---|---|---|
| | Bi2212 | Bi2223 | | | | | | | |
| 20 | 21.8 | 20.7 | 59.9±1.3 | 205±7 | 7.56 | 11.1 | 17.74 | 10.56 | 12500 |
| 50 | 24.1 | 24.4 | 72.9±2.9 | 273±10 | 7.54 | 11.37 | 17.05 | 11.04 | 15000 |
| 100 | 31.5 | 25.2 | 84.4±4.6 | 303±10 | 5.4 | 8.04 | 13.54 | 9.31 | 19000 |
| 150 | 65.4 | 27.2 | 87.0±4.1 | 383±13 | 6.13 | 9.12 | 16.24 | 12.25 | 20000 |

## Conclusion

This work demonstrates the efficient and reliable use of iterative combination of algorithms for structure (Rietveld), microstucture (Popa) and OD calculation (WIMV). Based on neutron diffraction, the combined approach was shown to be highly effective to extract texture strength, phase percentages and crystallite sizes in polyphased Bi2223 bulk superconducting materials. This new combined methodology is really innovative and promising to generalize the texture characterization of polycrystalline materials, to simplify the data treatment and to correlate anisotropic properties to texture strength, microstructure aspects…

## References

[1] H. M. Rietveld, *J. Appl. Cryst.* **2** (1969) 65-71

[2] S. Matthies, G. W. Vinel, *Physica Status Solidi B* **112** (1982) 111-120

[3] N. C. Popa, *J. Appl. Cryst.* **31** (1998) 176-180

[4] L. Lutterotti, S. Matthies, H.-R. Wenk, *Proceedings of the 20th International Conference on Textures of Materials*, Vol. 2, edited by J. A. Szpunar, (1999) 1599-1604. Montreal: NRC Research Press.

[5] E. Guilmeau, S. Lambert, D. Chateigner, J. G. Noudem, B. Ouladdiaf, *Mat.Sci.Eng. B* **104** (2003) 107-112

[6] H.-R. Wenk, L. Cont, Y. Xie, L. Lutterotti, L. Ratschbacher, J. Richardson, *J. Appl. Cryst.* **34** (2001) 442-453

[7] M. Morales, D. Chateigner, D. Fruchart, *J. Magn. Magn. Mater.* **257** (2003) 258-269

[8] M. Morales, D. Chateigner, L. Lutterotti, J. Ricote. *Mat. Sci. For.* **408-412** (2002) 113-118

[9] Y. Xie, H.-R. Wenk, S. Matthies, *Tectonophysics* **370** (2003) 269-286

[10] J-H. Bae, G. Heo, S. T. Oh, E. Shin, B-S. Seong, C-H. Lee, and K. H. Oh, *Mat. Sci. For.* **408-412** (2002) 215-220

[11] E. Guilmeau, D. Chateigner, J.G. Noudem, *Supercond. Sci. Technol.* **15** (2002) 1436-1444

[12] E. Guilmeau, D. Chateigner, J. Noudem, R. Funahashi, S. Horii, and B. Ouladdiaf, *Journal of Applied Crystallography* **38**, 2005, 199-210

[13] E. Guilmeau, D. Chateigner, J.G. Noudem, *Supercond. Sci. Technol.* **16** (2003) 484-491